

49th SME North American Manufacturing Research Conference, NAMRC 49, Ohio, USA

Parametrization of manual work in automotive assembly for wearable force sensing

Scott Kerner^{a,*}, Suryanarayanan Gunasekar^a, Rishabh Mulesh Vedant^a, Matthew Krugh^a,
Laine Mears^a

^aClemson University, 4 Research Dr., Greenville, SC 29607, USA

* Corresponding author. Tel.: +1-724-413-2007; E-mail address: scottkerner98@gmail.com

Abstract

This paper aims to model manual manufacturing processes by parameterizing operator force readings, specifically engine and coolant hose connections in an automotive assembly line. During automotive assembly, many processes are still performed manually by the human operator due to the complexity of automating the process or product with current technology. Processes include completing hose connections and subsequent "push-pull-push" verification testing. Manual work introduces an opportunity for human error because of the inconsistencies when completing tasks; even a slight variation in operation can lead to an incomplete or missed process. These incomplete processes can pass post-production checks, such as a pressure test, but later loosen and fail, causing rework or warranty issues. To minimize human error, operator force was parameterized to provide real-time feedback to the connection status. The operator force was chosen to classify connections and to verify testing quantitatively. The parametrization was completed by isolating the shear and normal forces using custom fixtures, with shear being the primary required force type. The varying finger and hand engagement for the different connector locations were factored into the parametrization to encompass a broader range of manually completed tasks. It was found that operator forces in finger engagement for manual assembly could be effectively represented by a limited set of measurable parameters.

© 2019 The Authors. Published by Elsevier B.V.

Peer review under the responsibility of the scientific committee of NAMRI/SME

Keywords: Manual assembly parametrization; parameterization; operator force classification; wearable force sensing; shear force; normal force

1. Introduction

This paper investigates three connector types utilized in joining engine hose components used as venting or fluid transfer lines. Due to the process flexibility needed, these operations are performed manually. This introduces the possibility of error while completing and checking the connections. Each of the connectors offers a click-type verification design that is audible but may go unnoticed in a noisy manufacturing environment; therefore, a coupled push-pull-push test is in place. The initial push completes the connection, the pull tests connection veracity, and the final push reseats the connection. This process is dependent on the forces applied by the operator and the proper completion of the process steps. Failure to properly perform this check can result in missed or incomplete connections causing rework if the error

is found during product testing or potential warranty issues if the product fails in the field.

This research aims to parameterize manual connections through forces applied to output the status of the connector to the operator. The parametrization provides numerical targets to the sensors used in measuring the operator forces. These force windows determine the likelihood of a successful connection as the operator force is applied. The primary contributing force investigated in the connection completion is a shear force with a less influential secondary normal force.

To establish an understanding of the forces exhibited by the operator in manual assembly, shear and normal force must be accounted for and differentiated for importance. Not all forces measured in manual operations contribute directly to the connection completion, but that does not mean that these forces are not necessary. For example, a normal force applied to the

hose or connector, which acts perpendicular to the direction of motion for connection completion, is needed to minimize slipping allowing for constant finger engagement. This creates a need for an understanding of the differentiation of the critical forces that are needed to physically mate the two connector halves and other forces indirectly contributing to the operation. Current shear force measurement devices are limited, leaving a gap in capability for measuring operator forces. A more capable form of operator shear force measurement is needed. Once the important forces are known, the operator target force envelopes can be established for the parametrization.

The manually performed task characterization utilizes inflection points in the force profiles to determine if the operator conducts the push-pull-push verification. It will also observe operator movements and approach to understand how the connection is completed. This will provide necessary information regarding applied force directions for the parametrization. The parametrization is a series of target force envelopes and the differentiation of multidimensional force signatures exhibited by the operator to understand the primary forces acting in the direction of the connector locking and additional measured forces acting in other directions.

The operator forces' successful parametrization will be used in production, providing real-time feedback to the worker as a source of task completion verification, classifying the assembly operations. These classifications can later act as a stepping stone for automating manually completed manufacturing processes by implementing the findings into autonomous systems to yield an automatic verification of the process.

Discussed in the following sections are an overview of the need for greater technology to complete manually performed assembly tasks and the state-of-the-art in wearable sensing and shear force sensing. This is followed by the experimental setup and procedure for measuring applied shear force through a series of custom fixtures with prototype sensors for the given connector types. An analysis of the observed data is then discussed with visuals and target force thresholds for completing each connection with statistical likelihood. Concluding remarks and future work follows.

2. Background

The probability of a human error occurring in manufacturing systems tends to increase as the workers gets farther into their shift. An experiment was conducted using historical data on non-compliance (rejected items and rework offline) directly attributed to man, with findings showing human error probability of 2-16% dependent on the task and elapsed time in the worker's shift [1]. As a result of human error, cost, and efficiency, recent efforts in manufacturing are moving towards the automation of repetitive tasks, providing an opportunity to create a societal change in manufacturing, "...improving the quality of life, raising productivity and earnings; making work less dirty, dangerous, physically punishing, and dull; and increasing the value of thinking, creativity, and expertise." [2]. Societal changes shape the automation of repetitive, manually completed tasks performed by workers in automotive production. However, many of these tasks are too complex to automate with existing robot technologies. Current robot

designs do not perform well in varying, unstructured environments with people and existing technology [2]. This is due to the knowledge gaps in robotics' adaptability and control when deviating from the programmed function. Robotics lack the flexibility to perform various manual processes because manipulation, mobility, and computation of current robotic technologies are customarily fixed processes [3]. Fixed processes meaning that robots are typically carefully designed and specified by fixed programming methods that cannot handle the process variability of manual automotive assembly.

Worker completed assembly offers a flexible format that can use reasoning and logic, increasing the potential of what the assembly line worker can determine [3]. This flexibility in workers can help ensure that variations from an ideal configuration in a production line do not majorly disrupt the production flow or lead to an incomplete or dysfunctional product. In automotive production, common manual tasks include hose connections, wire routing, and subsystem assembly. Much of the automotive production line assembly is performed by a human operator, generating the possibility of inconsistent or incomplete work.

A greater understanding of the product, process, and work system environment engaged in manually conducted tasks can be used to bridge the gap between manual work to collaborative manufacturing and collaborative to autonomy [4]. Quantifying characteristics in manual assembly requires perception and intelligent data interpretation [2], [5], [6]. These advancements can be achieved through greater sensing, vision, and cognition technologies [7]. To provide the necessary inputs for these technological advancements, parametrization and characterization of the manual work are needed. These parametrizations are also utilized for the calibration of solutions such as wearable sensing for automotive assembly. Such solutions will provide the operator with feedback on the process as it is completed ensuring all steps and verification of each step were completed.

Data about worker abilities, limitations, and variability must be quantified and applied to the design to improve compatibility between workers and product assembly [8]. The stronger the compatibility between the worker and the product being assembled, the greater the understanding of how the process is completed. Part of the solution to manual task classification is understanding the cycle of manual production processes through feedback of information on critical forces [9]. Active force readings based on the operator can yield the status of manually completed work in real-time.

Example applications demonstrated in this paper are hose connections and subsequent verification testing of connectors. These force readings can then be used to provide feedback to an operator or a robot giving subjective analytical contact detection [10]. As connections are manually completed, the operator applies a combination of normal and shear force to one half of the connector to join the two parts, with shear being the driving factor towards completing the connection. These force measurements can then be parameterized by creating target force windows and sample-based statistical probability to numerically prove the outcome of a connection. This yields the categorization of the connections and manual checks for review by the worker. Connectors categorized as incomplete can be

reinvestigated, ensuring the components are assembled correctly in initial assembly, minimizing future rework after leaving production rework and field failures.

3. Literature Review

In manufacturing, force sensors are encountered in machine monitoring, assembly-line production, and quality testing. Force sensing allows the manufacturer to monitor critical forces involved to verify the completion of a process or determine production components' health by determining force limits and targets. For example, force sensors can be found on machining equipment to detect when the machine, tool, or workpiece may be deviating from expected behavior. On the assembly line specifically, manufacturers are implementing sensing technologies into the human-driven tasks to increase the operator's physical, sensing, and cognitive capabilities [11]. Commonly force sensing is utilized, providing feedback such as finger activation and area of contact for the force [12]. This sensing can provide real-time data for the operator, decreasing human errors in the final product.

Sensor types developed for human tactile sensing can be classified as invasive and non-invasive forms. Invasive forms could be extreme, like a physical implant incorporated into a worker, or more moderate, like physical augmentative technology such as wearable sensing [13]. Non-invasive technology can also be a form of motion capture or audible signatures [9], [14].

Many sensors for augmenting human abilities utilized in manufacturing are capable of measuring normal force through capacitive or resistive materials. A relatively few sensors have documented findings showing the ability to measure shear force. Work has been conducted to develop and research sensor capabilities and applications with a recent focus on compacting sensor size and thickness for a less invasive solution, optimizing cost, and making the sensors more tractable [15]–[17]. There have been successful efforts in reducing sensor profiles, but the work is incomplete. Many efforts have looked towards the implementation of force sensing into a wearable sensing platform. Formats include a glove worn by the user to allow them to continue to perform work with minimal interference or inconvenience [9], [15], [16], [18], [19].

Advancements in the realm of measuring shear force acting between multiple surfaces or bodies effectively are much less complete than normal force sensing. Shear force sensors have been developed offering compact size, variable measurement, linear readings, and high sensitivity, but one that encompasses all attributes to a high degree does not exist [15]. Applications for these shear force sensors vary widely as well. A multi-axis sensor was developed to evaluate car seat comfort, which had a linear measurement with good sensitivity [20]. However, this design is not compact or thin enough for a glove application. Piezoresistive sensors have also been developed, which provide a highly sensitive measurement and quick response times, but fabrication techniques are costly [21]. 3D printed shear force sensors are another researched variation. Applications include thin, almost 2D designs or 3D layouts [22]. There is a need for a shear force sensor that can be used in a wearable format, that

is minimally invasive to avoid disruption to workers and possesses an acceptable working range and sensitivity.

4. Experimental Setup

Experiments were developed to correlate forces observed as the operator completes a connection into their shear and normal components. The experiments using force isolating fixtures will then be used to determine the force windows for each connector type to provide operator feedback on the connector status. The isolated forces will also be used in the calibration of the developed wearable shear force sensor.

To encompass a broad range of operator completed tasks in assembly, three engine component type connectors were investigated in this study. Each of these three types is utilized on multiple occasions in the final product. An example of each of these connector types can be seen in 1. Type 1, 2, and 3 transmit air for pollution filtration, gasoline, and act as a venting line, respectively. Three pairs (two mating halves for each pair) of each connector type mentioned above were utilized for the investigation to eliminate the risk of an abnormal connector exhibiting different properties or connection characteristics. Although multiples of these connectors are seen across the entire assembly, this is not representative of the manual work for all of assembly. However, methodologies and general parameters can be used towards characterizing other connector types or manual processes. Since the connectors are in multiple locations, associates use a multitude of grips triggering varying finger engagement. These grip variations result from the approach and body position, causing the operator ergonomics to vary with their level of reach and how the force is applied.

Fig. 1. Connector Types 1, 2, and 3 (left to right)

The two connector halves mate together by joining a male and female end, which is then locked in place by plastic clips that are automatically or manually engaged. When completing connections in production, the operator's grip style and

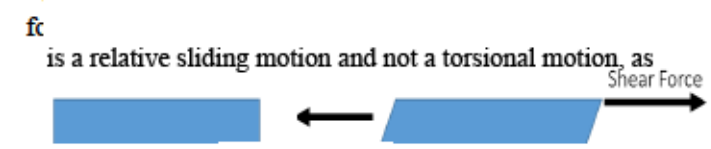
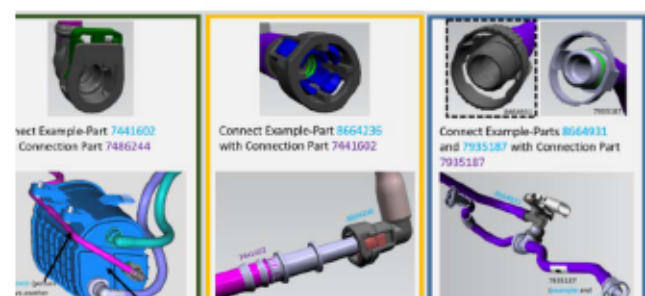
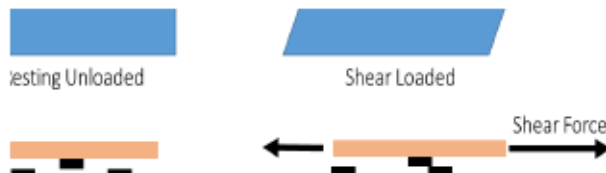


Fig. 2.





Since current literature and market products to measure this shear force in a wearable sensing format are limited, two fixtures were created to isolate and calibrate forces. An insertion force fixture measures the force acting on the connector to mate the two halves in one direction. The mating of the two halves can be performed at the desired speed via a servo motor or manually to mimic actual assembly. The shear force fixture measured the applied shear force by applying a known force to a block that can slide along a fixed axis.

4.1. Insertion Force Fixture

To measure normal force and calibrate the sensor glove, the insertion force fixture secured one-half of the investigated connectors to a sliding aluminium block that restricted motion in all directions except the x-direction, as seen in Fig. 3Fig. 4. Finger engagement demonstrating the utilization of shear force in grip. This allows the aluminium block to slide freely with the force sensor, recording the force in the x-direction while completing the connection. To understand the predominant force, the shear force, the data is first collected in terms of the normal force with the insertion force fixture. The insertion force needed to complete each connection can then be applied towards correlating the shear force necessary. As the operator grips the hose or connectors, a normal force is applied perpendicular to the x-direction, which keeps the fingers from slipping. The shear force is applied in the x-direction, which is the same direction that the force sensor measures data. The force sensor used in the study is a Mark-10 series 5i force indicator and series MR01-100 transducer with a dynamic range from 0.5 N to 10 kN [23].

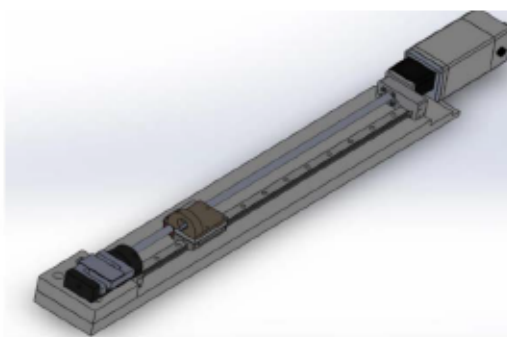


Fig. 3. Insertion force fixture setup

As the associate grips the half of the connector that is not secured, they utilize a grip that exhibits the shear force mentioned earlier, as seen in Fig. 4. The associate force acting on the connector is translated to the force sensor and recorded. This force is later used in conjunction with the developed shear force sensor to create the parametrization.

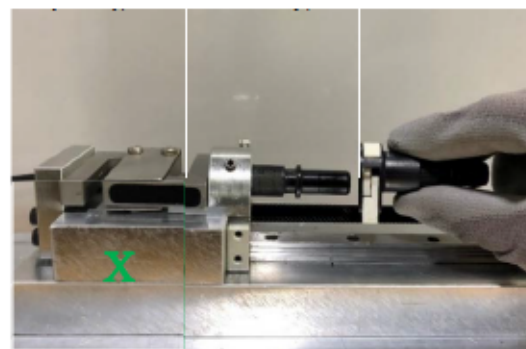
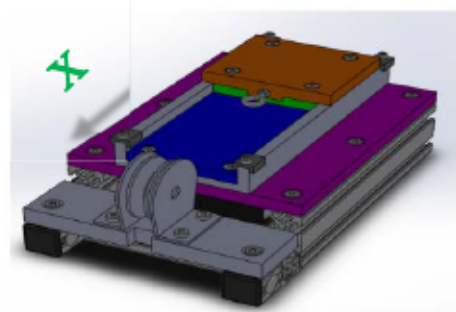


Fig. 4. Finger engagement demonstrating the utilization of shear force in grip

A series of tests were conducted across all three connector types with three replications of testing, using a new connector for each replication. The testing began with completing the connections using controlled speeds via a servo motor at 50 mm/s. This speed was selected to mimic the speed at which the assembler completes the connection. The servo motor utilized in testing is the Applied Motion Products TSM23S-3RG [24]. This allowed us to establish controlled baseline parameters for the force necessary to complete each connector type and a curve profile for each. Samples were collected at 250 Hz as this is the maximum sampling rate Matlab offers. From this, we moved on to the more variable, manually completed connection. Here, we tried to mimic the movements, speed, and timing of a production line associate. The manual connections were used to establish the initial push and characterize the connection push-pull-push check. To complete all tests, including the push-pull-push check, the aluminum block in the normal force fixture was secured to one side of the force sensor. The other end of the block was fixed, restricting movement in all directions. This allowed for the force sensor to flex and record forces acting on the connector and for a relative pushing and pulling motion to be completed.

4.2. Shear Force Fixture

To provide a preliminary understanding of the shear force, a shear force fixture was developed. This fixture isolated the applied shear force by applying a force only in the x-direction on a thin sensor design, as seen in Fig. 5. The sliding part of the fixture (orange and green, which are fixed together) moves along the blue plate by applying a known force to the block via a cord attached to the eyelet, seen in Fig. 5. This cord is drawn over the pulley only to act parallel to the relative motion, and weights are added to the cord's end. The displacement was also recorded to determine the operating range of the sensor.



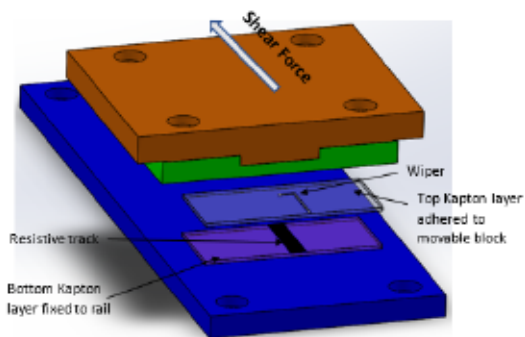


Fig. 5. Shear force fixture setup

The schematic of the developed shear force sensor can be seen in

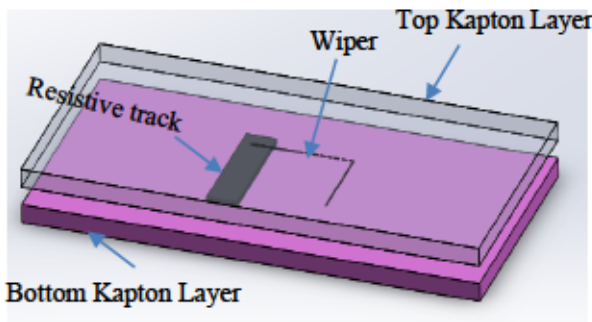


Fig. 6. The sensor relies on relative movement, exhibiting shear, of a conductive wiper along a resistive track. The top and bottom are attached to the sliding and fixed components of the shear force fixture by an adhesive to determine the shear force applied to the sensor and correlate it with resistance change. As the wiper moves along the resistive track when loaded in shear, the resistive output changes.

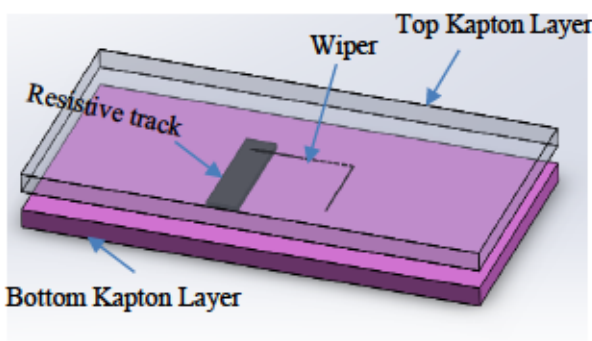


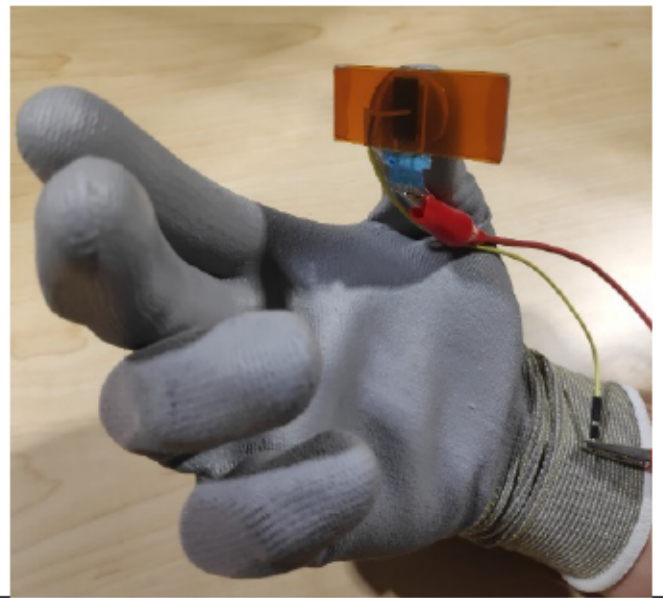
Fig. 6. Shear force resistive track sensor design

4.3. Sensor Glove Integration

Fig. 7 shows the functional sensor on the glove. It should be noted that the depicted sensor design and glove format are not in their final design format. Optimization of the sensor geometry, stability, and implementation into the glove was ongoing at the time of submission for the paper. However, the sensor's function remains the same, so the parametrization data is accurate.

Fig. 7. Shear force sensor and placement of the sensor on the glove

Table 1. Section 4 Testing Summary.



Test Type	Fixture Used	Object Tested	Test Repetitions for each Object	Total Number of tests
50 mm/s	Insertion force	3 connector types	20	180
Manual insertion	Insertion force	3 connector types	30	270
Shear sensor testing	Shear force	Sensor prototype		

5. Results and Analysis

An important assumption made for the insertion force data is that the force applied is in line with the sensor. This means there is no angular misalignment or linear offset, as depicted in Fig. 8. This ensures that the force applied to the connector is translated into the force sensor as an angular misalignment can be especially problematic due to only the force acting in the sensor direction is being recorded by the force sensor. There will be an x and y component to the force, but only the x will show.

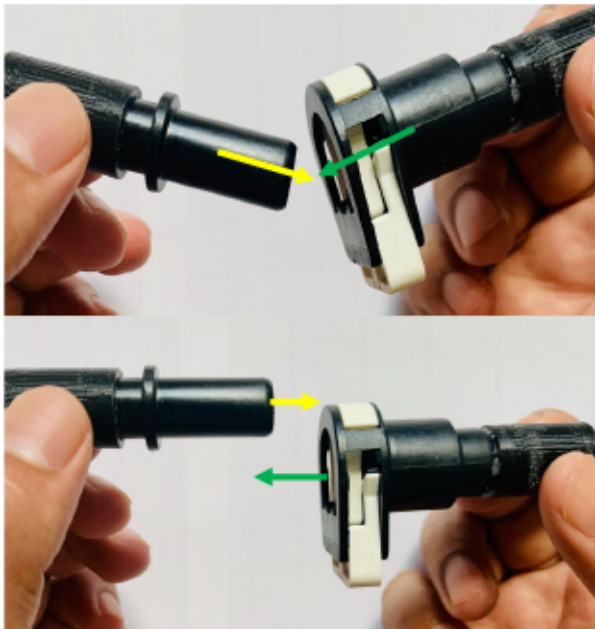


Fig. 8. Angular misalignment (top) and linear offset (bottom)

5.1. Controlled Speed

The speed of 50 mm/s was selected to imitate the speed at which the operator completes the connections. This baseline data was used to ensure the experimental setup's consistency to isolate forces while determining outside factors' influence versus the indiscriminate locking force needed to complete the connection.

The locking point for each connector type was established by utilizing camera footage concurrently to the force profiles. Customarily, the locking point for each force profile exhibited an upward or downward spike in force. Seen below in **Error! Reference source not found.** is the force profile over time for the Type 1 connector. As mentioned previously, three of each connector type were utilized in the investigation. This is the first pair for Type 1. Twenty tests were repeated with identical parameters, and each line indicates one of the twenty tests.

Each profile's locking point is centred around the zero point of the x-axis. This helped to compare the profiles to ensure consistency. The x-axis unit is time in seconds, and while it shows negative, this does not indicate a negative time. Since the locking points were centred around zero, the range of the scale for each connector should be recognized. It takes approximately 0.12 seconds for each connector to lock and an additional 0.045 seconds to seat, totalling an approximate connection completion time of around 0.165 seconds at a speed of 50 mm/s. The remainder of the force profiles for each connector type's remaining pairs are shown in Fig. 16-23 in section A.1 of the Appendix.

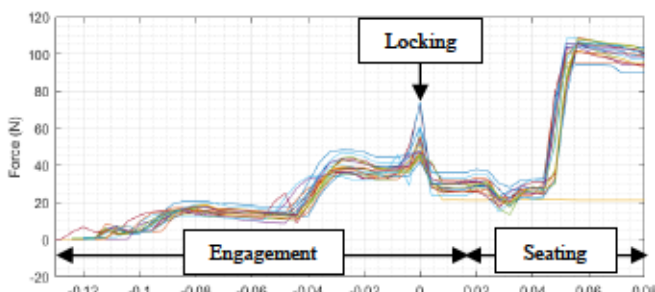


Fig. 9. Type 1, Pair 1 50 mm/s connection force profile over

We determined the parametrization of connector completion in controlled conditions and the connectors' degradation over time from this experimentation. The parametrization presented the target force needed for each connector type and the likelihood of a successful connection as force increases. This target force was used to ensure the manually completed connections were completed correctly by comparing the two sets of locking forces. As expected, the likelihood of a completed connection increases as higher forces are applied. A visualization of this is shown in Fig. 10. This graph encompasses all three pairs for the Type 1 connector. Critical points for plotting were established using the minimum, average, and maximum forces observed and benchmarks in increments of 10 to provide more data points. The remaining connection completion profiles are shown in Fig. 24 and 25 in section A.2 of the Appendix. The degradation properties of each connector type were observed by repeating the connection over hundreds of trials. It was found that the connectors exhibited no degradation in the completion force in the amount of time or number of tests conducted for this study. Therefore, the tests' order or the differentiation for each line in **Error! Reference source not found.** is insignificant because locking forces did not decrease or increase with time or use.

Fig. 10. Type 1 50 mm/s connection completion likelihood based on the force applied

5.2. Push-pull-push

The push-pull-push test is composed of three stages. The first stage is the initial push, which is the manual completion of the connection through locking and seating, similar to the force profile seen above for 50 mm/s. The second phase is the operator's pulling motion to verify the completion of the initial push phase's connection. The third phase, a secondary push, is a reseating of the connector to ensure the connector is in the optimal final position. A single force profile of the push-pull-push test can be seen below

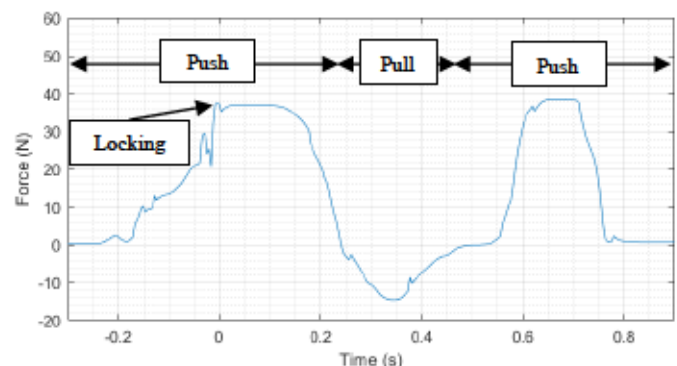


Fig. 11. The stages are divided by inflection points on the graph (when there is a sign change in force readings). Each stage is parameterized individually so it can be incorporated into a force measurement device for the operator.

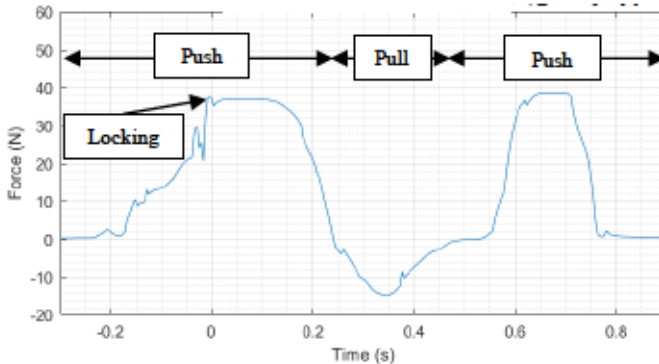
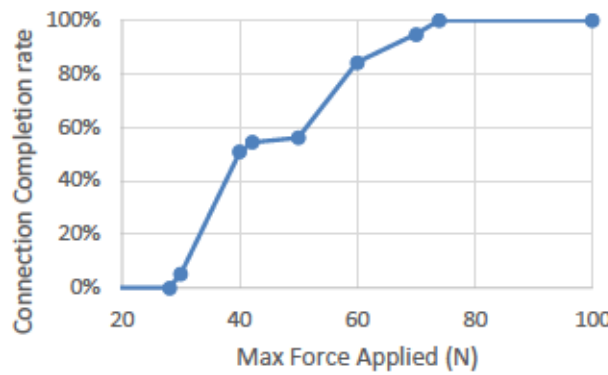


Fig. 11. Type 1, Pair 1 push-pull-push force profile over time (one test)

The complete 30 test profile is shown in Fig. 12. As mentioned before, the tests' order is insignificant because variation in the data is not due to degradation of the connector over time or as more connections are completed. The push-



pull-push phases, such as the ones indicated in

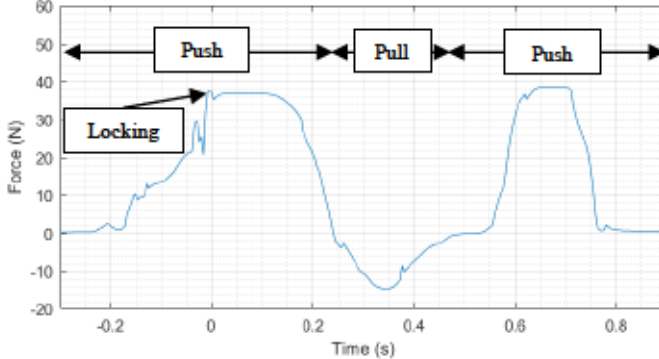


Fig. 11, continue to utilized inflection points as indication of a change in the applied force direction. The remaining push-pull-push force profiles for all types can be seen in Fig. 26-33 section A.3 of the appendix.

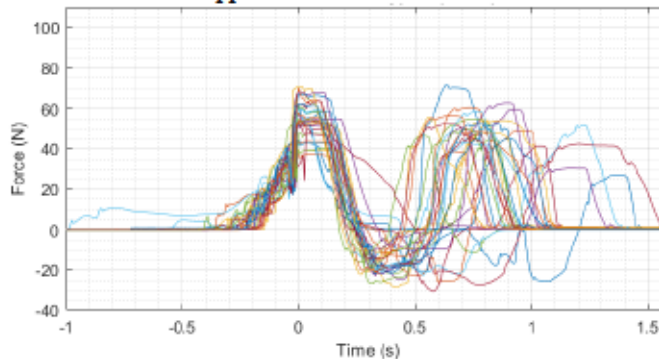


Fig. 12. Type 1, Pair 1 push-pull-push force profile over time (30 tests)

The push-pull-push parametrization utilized a similar approach to the parametrization for the 50 mm/s controlled speed. However, the initial push is the most critical that requires a more detailed look into the recorded forces. As stated before, the probability of a completed connection increases as the force applied increases. This likelihood is displayed in Fig. 13, which resembles a linear trend for the bulk of the data. The middle range is most critical for determining force as either side of this becomes closer to steady-state and is well below or above the force needed to complete the connection. This linear trend of the middle data, highlighted in red, will be used for calibration once the force sensors are applied in a format for operator use. All three types of connectors exhibit this linear trend, creating an efficient method for real-time operator feedback. The likelihood of a completed connection for the remaining two types are in section A.2 of the Appendix.

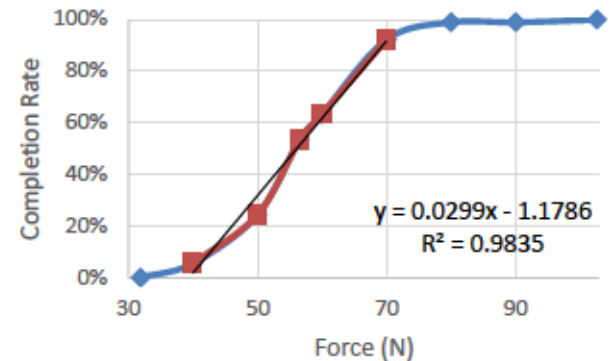


Fig. 13. Type 1 push-pull-push connection completion likelihood based on the force applied

Baseline target forces were established on a 90% success rate. These values apply to the initial push. The pull and secondary push data were operator dependent, establishing forces based on whatever "felt" sufficient for connection verification. These force values were lower than the force necessary or the forces observed for the first push. An average



of approximately 20 N and slightly below the initial push were seen for the pull and secondary push, respectively. Rather than requiring a specific force target for the pull and push 2 stages, the inflection points are utilized. This confirms that the operator completes the check. If a connection is completed successfully, these forces do not need to be large. The pull will separate the two connector halves relatively easily if the connection is unsuccessful. Table 1 below shows the characterization of the operator motion when completing any of the three connector types. These numbers can be adapted to reflect a greater probability of success.

Table 1. Characterization of the push-pull-push test

	Push 1	Pull	Push 2
Type 1	>69.52 N	<0 N	>0 N
Type 2	>120 N	<0 N	>0 N
Type 3	>80 N	<0 N	>0 N

Target values were set, and real-time feedback can be shown to the operator yielding the connector's status and the force profile or max force achieved. This is done by utilizing the output from the developed shear force sensor. As mentioned previously, the sensor has a resistive track in which a conductive wiper moves along as the shear force is applied. This change in resistance can be calibrated to the change in force, such as the profiles seen in Fig. 14.

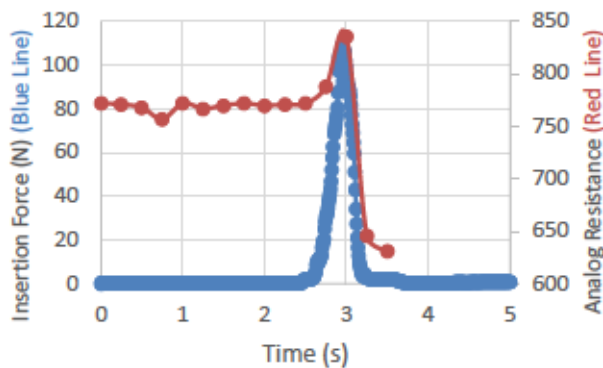


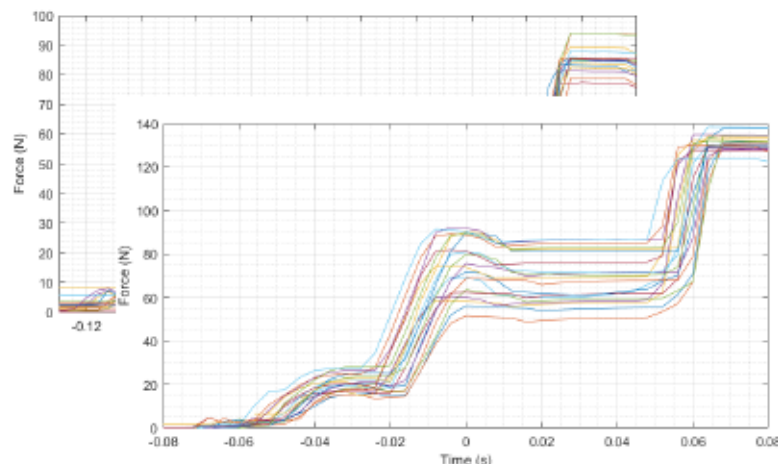
Fig. 14. Real-time operator feedback example insertion force and analog resistance profiles over time

As shown in Fig. 15, this setup utilized a grip with the sensor mounted on the thumb based on assembly line observations. The resistance profile in Fig. 14 shows a relatively constant value when the sensor is unloaded in shear but loaded in normal (i.e., the operator is gripping the hose). This slight fluctuation is due to noise and slight positional adjustments from the operator. The profile exhibits a positive change in resistance as the wiper moves along the track, which aligns with the insertion force change. After the connection is completed, the operator released the hose, which caused a momentary discontinuity between the track and wiper, causing the analog resistance readout to fall below the steady-state seen before the connection.

Fig. 15. Operator grip with the shear force sensor attached to the thumb on the glove

6. Conclusion

This paper's goal was to parameterize manually completed tasks by the worker in an automotive assembly environment, providing numerical targets to the sensors used in measuring the operator forces. This was done by monitoring the operator's forces to complete 3 connection types used in assembly. The



primary force utilized was a shear force with a secondary normal force. Force profiles over time were produced from the insertion force fixture, which was then attributed to the change in resistance in the developed shear force sensor.

The experimental work on operator forces was successfully parameterized for connection completion and subsequent verification testing through the push-pull-push. Results can be utilized for the implementation of wearable force-sensing devices, providing real-time operator feedback. This can be in the form of a force profile output or indication of target forces being met for the operation. This will minimize rework once the product leaves the manufacturing facility by verifying that manual assembly tasks are completed. The characterization of the manual work can also contribute to robots' calibration as repetitive tasks are automated in manufacturing.

Future research efforts can investigate sensor refinement to more accurately measure shear force with a repeatable, stable outcome. This will help direct another research path of a more detailed breakdown of applied forces and their proposed targets and thresholds. Continued efforts will contribute to the transition for collaborative manufacturing and Industry 5.0 robotics in manufacturing.

Appendix A. Force Profiles and Connection Probability

A.1. Controlled speed connection force profiles

Fig. 16. Type 1, Pair 2 50 mm/s connection force profile over time

Fig. 17. Type 1, Pair 3 50 mm/s connection force profile over time

Fig. 18. Type 2, Pair 1 50 mm/s connection force profile over time

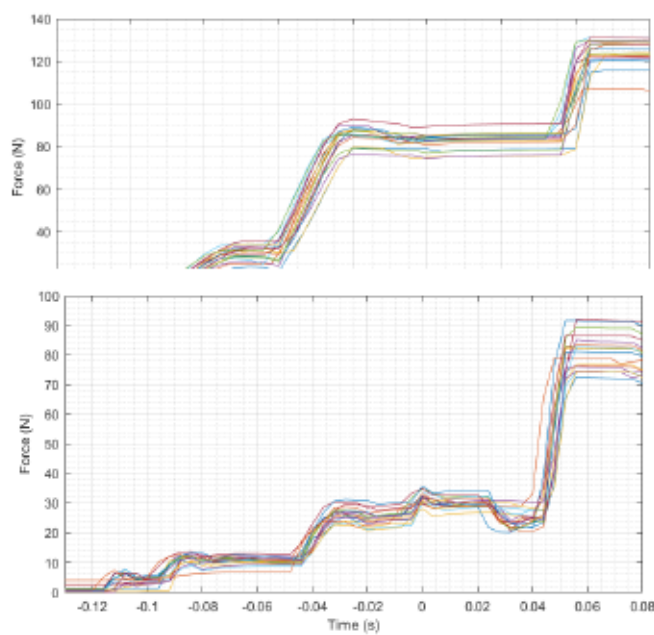


Fig. 19. Type 2, Pair 2 50 mm/s connection force profile over time

Fig. 20. Type 2, Pair 3 50 mm/s connection force profile over time

Fig. 21. Type 3, Pair 1 50 mm/s connection force profile over time

Fig. 22. Type 3, Pair 2 50 mm/s connection force profile over time

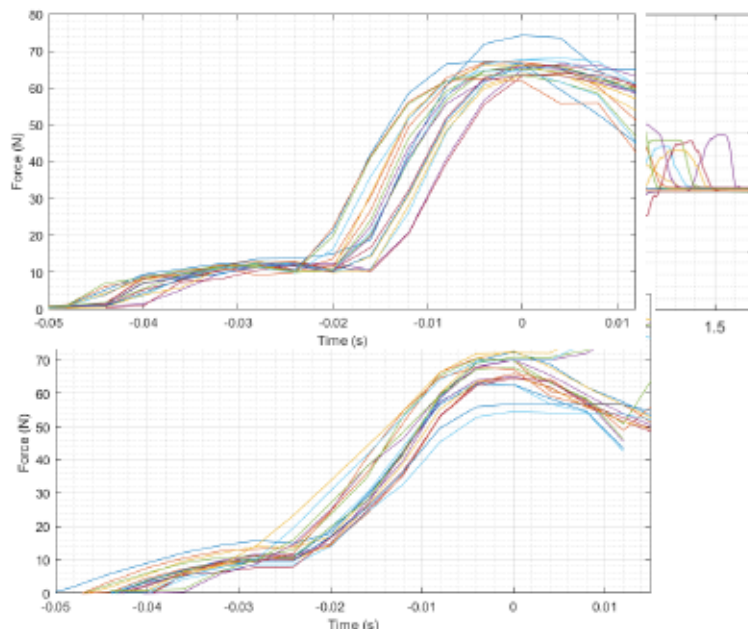
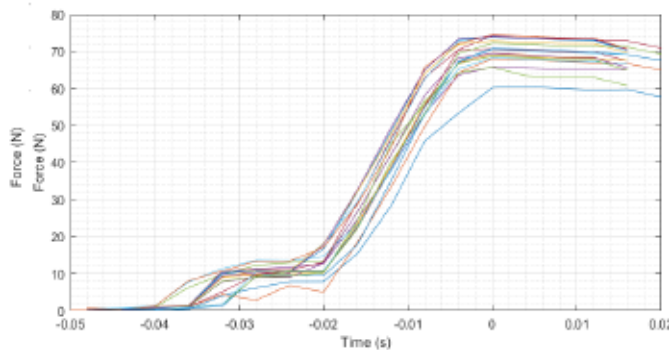


Fig. 23. Type 3, Pair 3 50 mm/s connection force profile over time

A.2. Likelihood of a successful connection

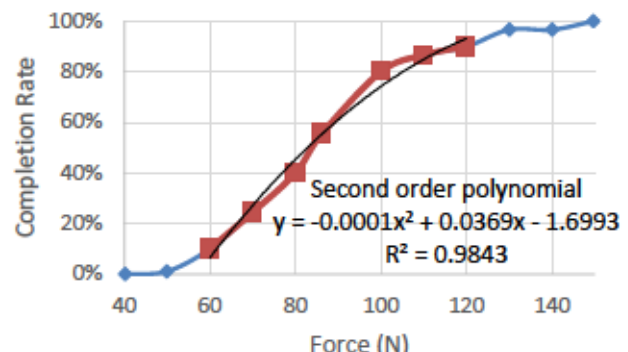


Fig. 24. Type 2 Connection Completion Rate vs Max Force

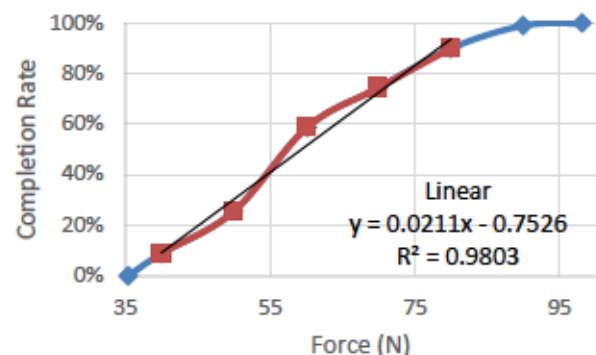


Fig. 25. Type 3 Connection Completion Rate vs Max Force

A.3. Push-pull-push force profiles

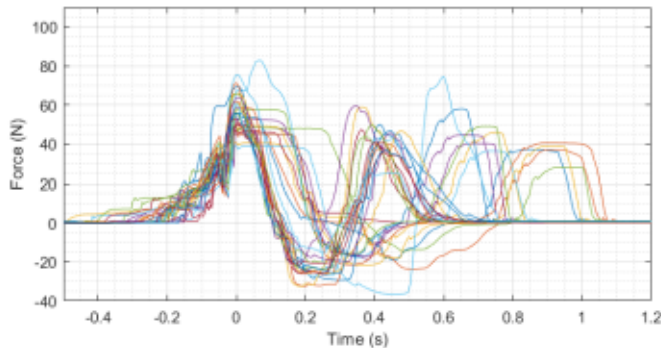
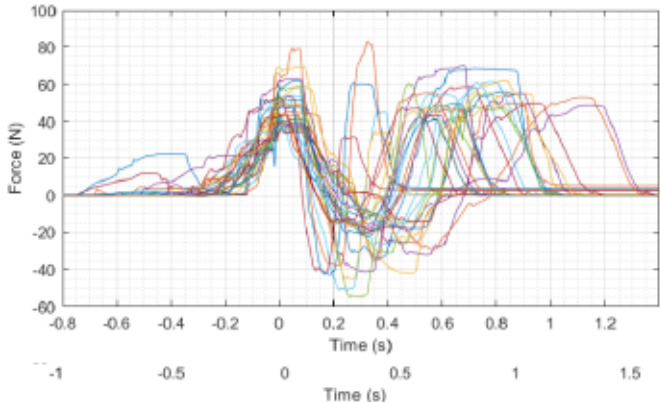
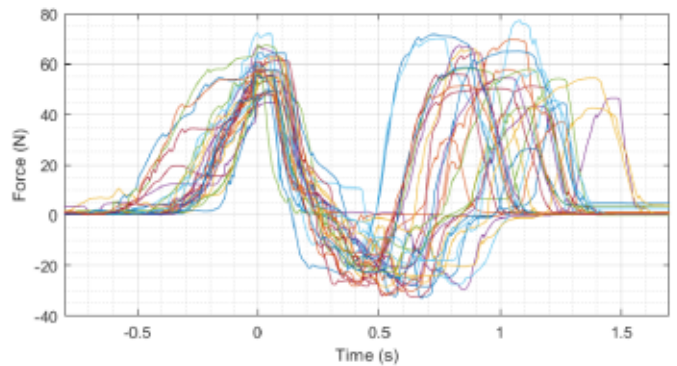


Fig. 26. Type 1, Pair 2 push-pull-push connection force profile over time

Fig. 26. Type 1, Pair 3 push-pull-push connection force profile over time

Fig. 27. Type 2, Pair 1 push-pull-push connection force profile over time

Fig. 28. Type 2, Pair 2 push-pull-push connection force profile over time



References

- [1] V. Di Pasquale, C. Franciosi, A. Lambiase, and S. Miranda, "Methodology for the analysis and quantification of human error probability in manufacturing systems," 2017, doi: 10.1109/SCORED.2016.7810093.
- [2] G. Stratton-Porter, "The Work of the Future: Shaping Technology and Institutions," 2018.
- [3] L. Miller, "Factory of the Future," in *Industrial Management & Data Systems*, vol. 84, no. 1–2, 2019, pp. 16–18.
- [4] A. Hengstebeck, K. Weisner, M. Klöckner, J. Deuse, B. Kuhlenkötter, and J. Rößmann, "Formal Modelling of Manual Work Processes for the Application of Industrial Service Robotics," in *Procedia CIRP*, 2016, vol. 41, doi: 10.1016/j.procir.2015.12.013.
- [5] M. Bortolini, M. Faccio, F. G. Galizia, M. Gamberi, and F. Pilati, "Design, engineering and testing of an innovative adaptive automation assembly system," *Assem. Autom.*, vol. 40, no. 3, 2020, doi: 10.1108/AA-06-2019-0103.
- [6] Subcommittee on Advanced Manufacturing of the National Science and Technology Council, "Strategy for American Leadership in Advanced Manufacturing," *Natl. Sci. Technol. Coun.*, no. October, pp. 1–40, 2018, [Online]. Available: papers3://publication/uuid/C7139B46-00F5-4E25-B13D-9E4A05DCCE6E.
- [7] L. Xu and F. Yu, "Factors that influence robot acceptance," *Kexue Tongbao/Chinese Sci. Bull.*, vol. 65, no. 6, 2020, doi: 10.1360/TB-2019-0136.
- [8] M. Reinvee and K. Jansen, "Utilisation of tactile sensors in ergonomic assessment of hand-handle interface: A review," *Agron. Res.*, vol. 12, no. 3, 2014.
- [9] T. Sagisaka, Y. Ohmura, A. Nagakubo, Y. Kuniyoshi, and K. Ozaki, "High-density Conformable Tactile Sensing Glove," *J. Robot. Soc. Japan*, vol. 30, no. 7, 2012, doi: 10.7210/jrsj.30.711.
- [10] G. H. Büscher, R. Köiva, C. Schürmann, R. Haschke, and H. J.

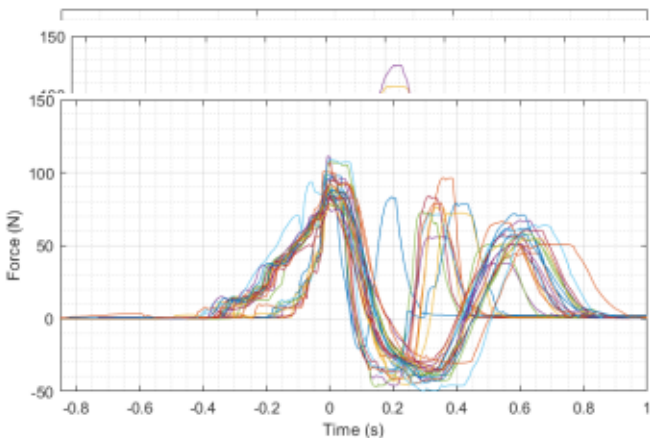


Fig. 29. Type 2, Pair 3 push-pull-push connection force profile over time

Fig. 30. Type 3, Pair 1 push-pull-push connection force profile over time

Fig. 31. Type 3, Pair 2 push-pull-push connection force profile over time

Fig. 32. Type 3, Pair 3 push-pull-push connection force profile over time

Ritter, "Flexible and stretchable fabric-based tactile sensor," *Rob. Auton. Syst.*, vol. 63, pp. 244–252, Jan. 2015, doi: 10.1016/j.robot.2014.09.007.

[11] I. Zolotová, P. Papcun, E. Kajáti, M. Miškuf, and J. Mocnej, "Smart and cognitive solutions for Operator 4.0: Laboratory H-CPPS case studies," *Comput. Ind. Eng.*, vol. 139, 2020, doi: 10.1016/j.cie.2018.10.032.

[12] M. Krugh, R. M. Vedant, R. S. Garimella, A. Baburaj, E. Wescoat, and L. Mears, "Associate finger engagement during manual assembly in automotive production for smart wearable systems," in *Procedia Manufacturing*, 2019, vol. 39, doi: 10.1016/j.promfg.2020.01.332.

[13] V. G. Macefield, C. Häger-Ross, and R. S. Johansson, "Control of grip force during restraint of an object held between finger and thumb: Responses of cutaneous afferents from the digits," *Exp. Brain Res.*, vol. 108, no. 1, 1996, doi: 10.1007/BF00242913.

[14] K. S. Lee and M. C. Jung, "Investigation of hand postures in manufacturing industries according to hand and object properties," *Int. J. Ind. Ergon.*, vol. 46, 2015, doi: 10.1016/j.ergon.2015.01.001.

[15] J. Mertodikromo, F. Zorin, and C. J. Lee, "A Low-Profile Shear Force Sensor for Wearable Applications," *IEEE Sens. J.*, vol. 20, no. 18, 2020, doi: 10.1109/JSEN.2020.2985396.

[16] F. L. Hammond, Y. Menguc, and R. J. Wood, "Toward a modular soft sensor-embedded glove for human hand motion and tactile pressure measurement," 2014, doi: 10.1109/IROS.2014.6943125.

[17] S. Cramp, C. MacColl, and R. B. Wallace, "Preliminary results for novel shear force sensor using force sensitive resistors," 2020, doi: 10.1109/T2MTC43012.2020.9128858.

[18] G. H. Büscher, R. Köiva, C. Schürmann, R. Haschke, and H. J. Ritter, "Flexible and stretchable fabric-based tactile sensor," *Rob. Auton. Syst.*, vol. 63, no. P3, 2015, doi: 10.1016/j.robot.2014.09.007.

[19] A. Polishchuk, W. T. Navaraj, H. Heidari, and R. Dahiya, "Multisensory Smart Glove for Tactile Feedback in Prosthetic Hand," in *Procedia Engineering*, 2016, vol. 168, doi: 10.1016/j.proeng.2016.11.471.

[20] S. G. Kim et al., "Development of a shear force measurement dummy for seat comfort," *PLoS One*, vol. 12, no. 11, 2017, doi: 10.1371/journal.pone.0187918.

[21] S. M. Won et al., "Multimodal Sensing with a Three-Dimensional Piezoresistive Structure," *ACS Nano*, vol. 13, no. 10, 2019, doi: 10.1021/acsnano.9b02030.

[22] C. Liu et al., "3D printing technologies for flexible tactile sensors toward wearable electronics and electronic skin," *Polymers*, vol. 10, no. 6, 2018, doi: 10.3390/polym10060629.

[23] R. Koiva, B. Hilsenbeck, and C. Castellini, "FFLS: An accurate linear device for measuring synergistic finger contractions," 2012, doi: 10.1109/EMBC.2012.6345985.

[24] "TSM23S-3RG | Applied Motion." <https://www.applied-motion.com/products/stepperservos-integrated-motors/tsm23s-3rg> (accessed Nov. 19, 2020).